

Chalcogenide glass e-beam and photoresists for ultrathin grayscale patterning

Andriy Kovalskiy
Jiri Cech

Lehigh University
Center for Optical Technologies
5 East Packer Avenue
Bethlehem, Pennsylvania 18015
E-mail: ank304@lehigh.edu

Miroslav Vlicek

University of Pardubice
Faculty of Chemical Technology
nam. Cs. legii 565
53210 Pardubice, Czech Republic

Christopher M. Waits
Madan Dubey

Army Research Laboratory
Sensors and Electron Devices Directorate
2800 Powder Mill Road
Adelphi, Maryland 20783-1197

William R. Heffner

Himanshu Jain
Lehigh University
International Materials Institute for New
Functionality in Glass
7 Asa Drive
Bethlehem, Pennsylvania 18015

Abstract. The advantages and applications of chalcogenide glass (ChG) thin film photoresists for grayscale lithography are demonstrated. It is shown that the ChG films can be used to make ultrathin (~ 600 nm), high-resolution grayscale patterns, which can find their application, for example, in IR optics. Unlike polymer photoresists, the IR transparent ChG patterns can be useful as such on the surface or can be used to transfer the etched pattern into silicon or other substrates. Even if the ChG is used as an etch mask for the silicon substrate, its greater hardness can achieve a greater etch selectivity than that obtained with organic photoresists. The suitability of ChG photoresists is demonstrated with inexpensive and reliable fabrication of ultrathin Fresnel lenses that are transparent in the visible as well as in the IR region. The optical functionality of the Fresnel lenses is confirmed. Application of silver photodissolution in grayscale lithography for microelectromechanical systems (MEMS) applications is also shown. A substrate to ChG/silver thickness etching ratio of ~ 10 is obtained for the transfer of patterns into silicon using reactive ion etching (RIE), more than a fivefold increase compared to traditional polymer photoresist. © 2009 Society of Photo-Optical Instrumentation Engineers. [DOI: 10.1117/1.3273966]

Subject terms: chalcogenide glass (ChG); photoresist; gray scale; lithography; Fresnel lenses; dry etching; wet etching.

Paper 09118PR received Jun. 30, 2009; revised manuscript received Oct. 14, 2009; accepted for publication Oct. 23, 2009; published online Dec. 22, 2009.

1 Introduction

Advanced grayscale photo- and electron-beam lithography allows the creation of continuous multilevel surface relief micro- and nanostructures and is commonly used in microoptics, micro/nanoelectromechanical systems (MEMS/NEMS), and biomedical devices.^{1–4} Most of the grayscale lithography processes are based on conventional planar lithography resists, typically polymers. Grayscale lithography using polymer photoresists has been successful for making large-area gradient profiles with the aim of further transfer to a substrate, usually silicon, with reactive ion etching (RIE)⁵ or deep reactive ion etching (DRIE).⁶ For example, phase Fresnel lenses developed on polymer photoresists with initial pattern height of $3 \mu\text{m}$ could be transferred into silicon with the appropriate phase shift at each point on the lens with a DRIE etch selectivity of 15:1 (Ref. 6). Another promising advanced method for the development of relatively thin Fresnel lenses ($\sim 4 \mu\text{m}$) was proposed using a binary optics technique.⁷

The transfer of patterns into silicon may not always be needed or even desirable, especially when the photoresist itself may work as an optical component (e.g., a refracting

surface). A 3-D optical element patterned through a grayscale mask on the right resist material may itself possess the required optical properties,² thus simplifying the device structure and fabrication considerably. The direct application of the patterned resists could significantly reduce the cost and time of fabrication as well. Different types of glass resists [sol-gel,² chalcogenide glasses (ChG)⁸], which are much harder than polymers, are often proposed for such applications. Moreover, polymers are not always suitable for ultrathin and nanosize structures, when one needs a resist material that is highly sensitive to irradiation, easily structured on the nanoscale, and hard enough to be used as the object/structural material or transferred into silicon substrate. In this paper, we propose ChG thin film photoresists as prospective materials to produce ultrathin (~ 600 nm) grayscale patterns. They are also expected to yield better control of the geometry than is possible with polymer resists. Our materials have an additional remarkable property of radiation-induced diffusion of silver, which opens new opportunities for grayscale lithography. Light, x-ray, or e-beam irradiation causes complete dissolution of thin (up to ~ 50 nm) silver layer deposited on top of a ChG film, gradually changing the chemical resistance of the latter depending on the time and intensity of irradiation and thickness of the silver layer.⁹

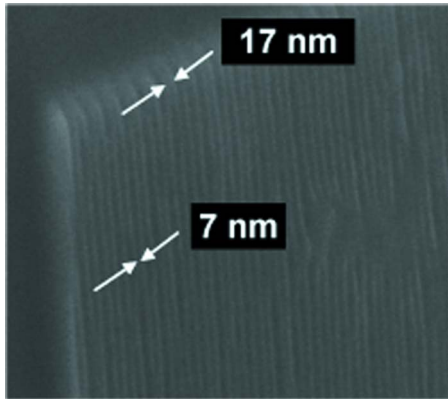


Fig. 1 SEM pictures of e-beam patterned and wet-etched $\text{As}_{35}\text{S}_{65}$ ChG thin film: line separation ~ 7 nm, width ~ 17 nm, and height ~ 80 nm.

2 Properties of Chalcogenide Glass Photoresists

Thin films of ChG (alloys of S, Se, and Te with more positive elements) possess the unique ability to change their structure under the influence of light (UV, visible radiation with an energy greater than or equal to the bandgap of the ChG layer),¹⁰ x-rays,¹¹ and electrons.¹² The photo-induced patterning on ChG can be realized with different maskless technologies (direct writing with deep ultraviolet,¹³ visible¹⁴ or femtosecond laser^{15,16} radiation, and holographic recording¹⁷) or using binary and grayscale mask lithographic methods.^{8,9}

The films investigated in this work are prepared by conventional thermal evaporation in vacuum. Structurally, most of the ChG films can be considered as rigid polymers having a network-like structure but without large molecular units. For such a thin film structure, the smallest feature size that can be patterned is determined by the type of irradiation, not the resist itself. Features of ~ 7 nm spaces and 17-nm lines, apparently the finest structure made in a glass (Fig. 1), have been fabricated in our laboratory by exposing $\text{As}_{35}\text{S}_{65}$ thin film to low-energy electron beam followed by wet etching in amine solution.¹⁸ Figure 2 clearly shows well-resolved spots at the 10-nm scale on an e-beam irradiated surface of As_2S_3 thin film. Although the beam can be focused to 1-nm spot, the minimum feature size and resolution has been larger than this value. Both the

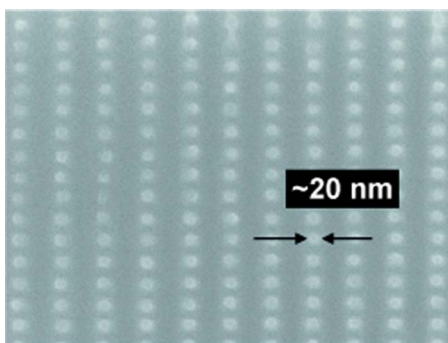


Fig. 2 Demonstration of the separate e-beam spots on the surface of wet-etched electron-irradiated As_2S_3 ChG thin film.

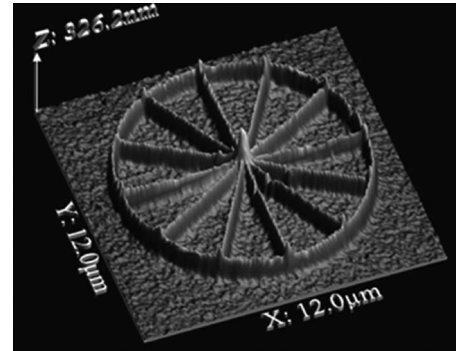


Fig. 3 3-D AFM picture of "nanospokes."

Gaussian intensity profile of the electron beam and the secondary electrons produced well outside the region of primary exposure cause the width of etched lines to be significantly larger than the diameter of the writing e-beam itself.

Previously, we demonstrated also the fabrication of complex grayscale patterns with 3-D topology on chalcogenide glasses using electron-beam lithography tools.¹⁹ For instance, to establish the fidelity of patterning and the ability to form grayscale features, we formed a wheel-shape structure, as shown in Fig. 3 (diameter $\sim 10 \mu\text{m}$ and line-width ~ 200 nm). The radial lines were written following the circle. Notice the greater height of etched structure due to higher electron dose, where the lines intersect each other. A quantitative correlation between the total electron dose and feature height is shown in Fig. 4. The height of the etched structure depends linearly on the dose of electron irradiation. Such linear dependence is an important consideration for ultrafine e-beam grayscale lithography.

In addition to higher resolution, ChG thin films may have several other advantages over polymers, such as higher durability under reactive ion etching and higher resistance to acids.²⁰ They are suitable for selective etching of SiO_2 , Si, Cr, etc., which are used in microelectronic and MEMS processing.²¹ It is also important to note that the pre-baking and post-baking steps of polymer-based lithography are completely eliminated. Moreover, by simply changing the composition of the wet developer,²² or even

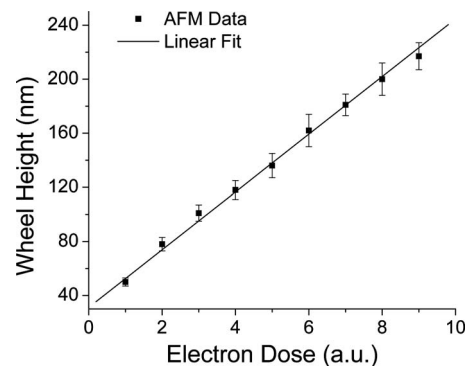


Fig. 4 Thickness of the As-S thin film remaining after etching versus electron dose. Experimental points represent heights of differently exposed regions of structures such as those shown in Fig. 3.

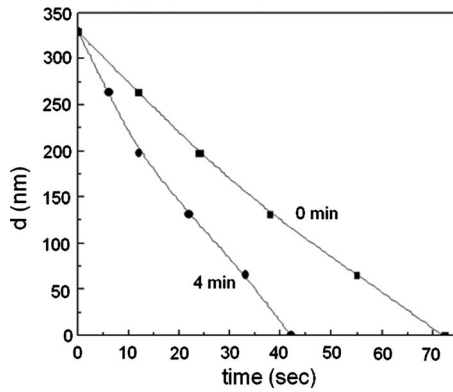


Fig. 5 Kinetics of dissolution of as-evaporated and 4-min exposed As_2S_3 film ($d_0=330$ nm) in aqueous solution of $\text{Na}_2\text{CO}_3+\text{Na}_3\text{PO}_4$ (positive etching).

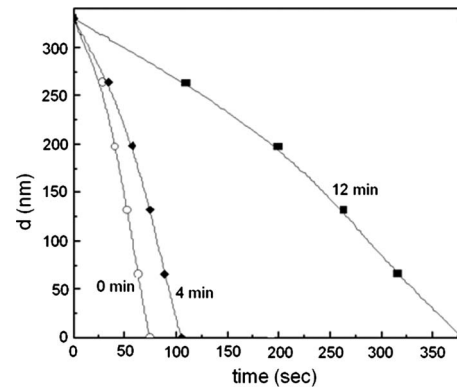


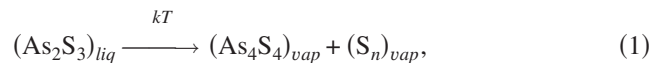
Fig. 6 Kinetics of dissolution of as-evaporated and different time exposed $\text{As}_{35}\text{S}_{65}$ film ($d_0=330$ nm) in nonaqueous amine-based solution (negative etching).

time of etching²³ or substrate temperature,²⁴ certain chalcogenide glass can be used as both a positive and a negative photoresist.

An example of such dual behavior has been demonstrated on thin films of stoichiometric As_2S_3 , which can serve as a positive or negative photoresist depending on the alkaline developer used.²⁵ The kinetics of As_2S_3 thin film dissolution (positive etching) in the aqueous solution $\text{Na}_2\text{CO}_3+\text{Na}_3\text{PO}_4$ is presented in Fig. 5. With nonaqueous, amine-based solvents, an As-based ChG film usually behaves as a negative resist (Fig. 6). The latter is mostly used for grayscale patterns like optical lenses.²⁶ Furthermore, ChG could also be negatively etched in plasma containing the gas mixtures of CF_4 , Ar, and O_2 .²⁷

The mechanism of selective etching follows from the structural features of as-prepared ChG thin films. Bulk stoichiometric ChG such as $\text{As}_2(\text{S},\text{Se})_3$ and $\text{Ge}(\text{S},\text{Se})_2$ consist of pyramidal $\text{As}(\text{S},\text{Se})_{3/2}$ or tetrahedral $\text{Ge}(\text{S},\text{Se})_{4/2}$ structural units, respectively. Homopolar bonds in such glasses are possible, in principle, only upon deviation from stoichiometry. However, as-prepared ChG thin films, even of stoichiometric compositions, contain a considerable fraction of “wrong” (the bonds which should not exist in bulk glasses of stoichiometric compositions) homopolar bonds (As-As, S-S, Se-Se, Ge-Ge). Concentration of such “wrong” bonds in the structure of as-evaporated films can vary from a few % to more than 10%, depending on the conditions of thermal evaporation, and can be consequently changed by exposing to radiation. Let us examine this difference by com-

paring the structure of bulk ChG, as-evaporated, and exposed thin film ChG (which is responsible for selective etching) of the stoichiometric As_2S_3 . In principle, only AsS_3 pyramidal units should form the structure of stoichiometric As_2S_3 . (Each sulfur must be corner-shared between two neighboring AsS_3 pyramids.) Raman spectra of the bulk ChG confirm validity of this concept—there the dominant broad band at 345 cm^{-1} corresponds to the presence of AsS_3 pyramids [Fig. 7(a)]. This band is slightly modified by shoulders at 312 and 380 cm^{-1} , which are assigned to the interactions between these AsS_3 pyramids. In contrast, the Raman spectra of as-evaporated thin film ChG [Fig. 7(b)] show very intense bands between 135 cm^{-1} and 234 cm^{-1} and also at 363 cm^{-1} , which can be assigned to the vibration of As-As containing units,²⁸ such as As_4S_4 , together with additional relatively strong double bands with maxima at 495 cm^{-1} and 474 cm^{-1} . These two bands are evidence that S-S containing structural units such as $-\text{S}-\text{S}-$ chains (495 cm^{-1}) and S_8 rings (474 cm^{-1}) are present and connect individual AsS_3 pyramids.^{29,30} The appearance of these structural units containing homopolar bonds in the structure of as-evaporated As_2S_3 thin films can be explained by the following thermal dissociation reaction during evaporation³¹:



where the nonstoichiometric As_4S_4 unit contains a homopolar As-As bond. Due to fast condensation of vapors on the

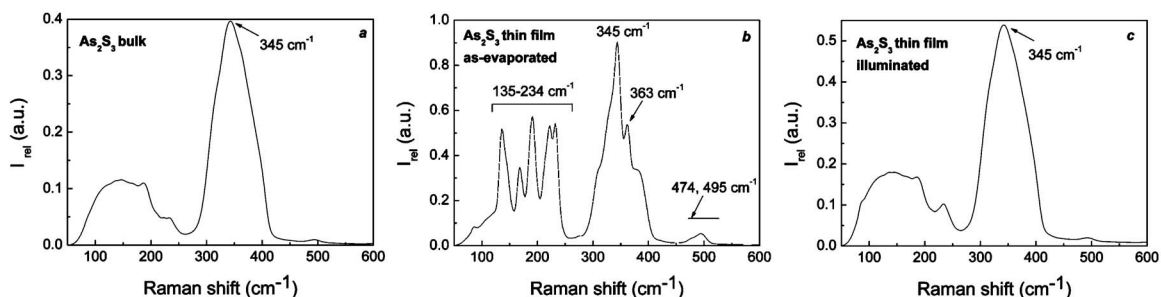


Fig. 7 Raman spectra of As_2S_3 samples: (a) bulk, (b) as-evaporated thin film, and (c) thin film after 30-min exposure with halogen lamp.

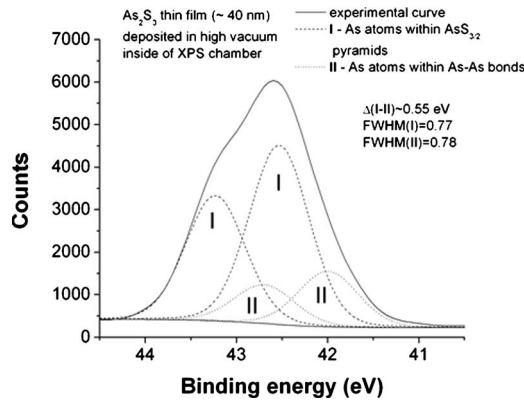


Fig. 8 Fitting of As 3d XPS core-level spectrum of as-evaporated As_2S_3 thin film

cold substrate (room temperature), these structural units are frozen in the structure of as-evaporated films and they are responsible for the photosensitivity of these films.²⁵

High-resolution x-ray photoelectron spectroscopy (XPS) can provide an accurate value for the concentration of atoms in different chemical states. One can easily estimate the concentration of homopolar bonds from the areas of appropriate components of fitted XPS core-level spectra. As an example, the XPS data for S 2p and As 3d core-level spectra for an As_2S_3 thin film are presented in Figs. 8 and 9. Areas I and II determine the concentration of atoms involved in heteropolar and homopolar bonds, respectively. The change in chemical resistance is a result in structural transformations caused by band-gap light or electron irradiation of as-prepared films and is dependent on the type and intensity of irradiation, chemical composition, and surface structure of the films. The relative concentration of the homopolar bonds is one of the key factors in the mechanism of these structural transformations.^{25,31}

The mechanism of selective wet etching of As_2S_3 thin films (and other As-based chalcogenides) in aqueous alkaline solutions is based on the different dissolution rates of AsS_3 pyramids, fragments with S-S homopolar bonds, and As_4S_4 structural units with As-As homopolar bonds.³² Concentration of homopolar bonds, which is high in the structure of as-evaporated films, is reduced by exposure to ra-

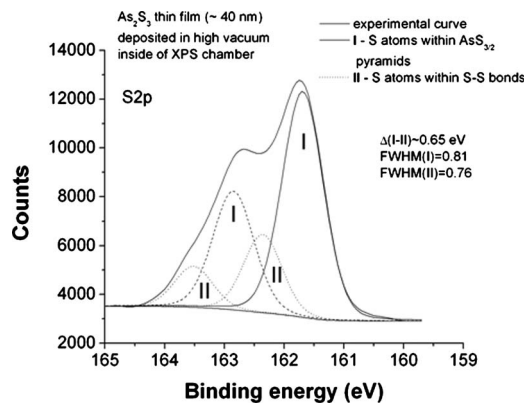


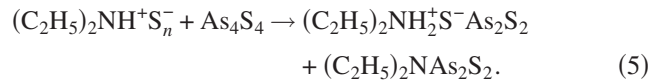
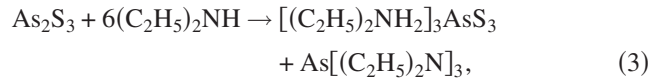
Fig. 9 Fitting of S 2p XPS core-level spectrum of as-evaporated As_2S_3 thin film.

diation, and the structure of the thin film becomes closer to the structure of bulk glass. Notice the significant drop in the intensity of bands between 135 and 234 cm^{-1} , at 363 cm^{-1} , 474 cm^{-1} and 495 cm^{-1} , in Fig. 7(c) in comparison with Fig. 7(b) after light illumination of the film due to the following polymerization reaction:⁸



leading to the change of chemical resistance.²⁵ The chemical reactions during etching of as-evaporated and exposed films have different kinetics, thereby resulting in selective positive etching, as described elsewhere.³²⁻³⁴ Another probable chemical reaction influencing the selective etching efficiency is arsenic photo-oxidation on the surface of ChG thin film.³⁵

Some authors³⁶ found negative selective etching of chalcogenide glass films in aqueous alkaline solvents. In this case, especially in chalcogen-rich compositions, the mechanism of dissolution is completely different due to the oxidation of As^{III} arsenic to As^{V} by polysulfide anions formed during the dissolution process in the etching bath and results in a negative type of etching, which is typical when amine-based solvents are applied as described in the following. Negative resist behavior of As_2S_3 thin films in amine-based solvents can be described by the following reactions for the As_2S_3 , As_4S_4 and S_n structural units:²⁸



The negative character of the etching in amine-based solvents is explained by the faster rate of reactions (4) and (5) in comparison to reaction (3).³¹

RIE of ChG can be performed using different gas chemistries. The RIE method consists of two processes: spontaneous chemical reaction, which improves etching selectivity, and physical sputtering, which lowers selectivity between the materials. The first comprehensive study of RIE of As_2S_3 thin films showed that pure CF_4 plasma is highly isotropic, causing unwanted undercutting of the film, and if too aggressive, causing very rough sidewalls.²⁷ The isotropic behavior of CF_4 was greatly reduced using O_2 and Ar additives to provide *in situ* passivation, with O_2/CF_4 having the best performance. Previous results of RIE of ChG show that good wall inclination angles (70 deg for CF_4/O_2 and 60 deg for CF_4 atmospheres, respectively) can be obtained.³⁷

The Ge-based ChG film photoresists consist of more rigid tetrahedral molecular units of larger size, which may limit their application in grayscale and nanoscale photolithography. Strong Ge oxidation is another poorly regulated factor, which may adversely affect their lithographic applications. However, it was shown that these materials could be successfully utilized for ion-beam lithography.^{38,39} Also

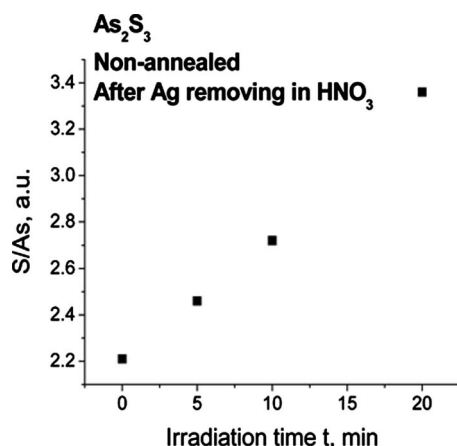
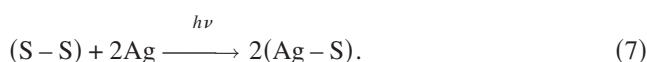
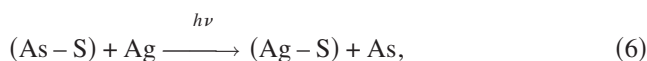


Fig. 10 XPS data on change of surface composition of the irradiated part of Ag/As₂S₃ sample with time of irradiation after development in dilute HNO₃.

they can be quite useful for the patterning based on controlled silver dissolution into ChG thin film, as described next.

The photo-induced silver dissolution can be used for fabricating 3-D grayscale masks in advanced MEMS and microelectronic technologies.⁹ The smooth 3-D microstructures in the ChG film can be transferred to Si by dry etching more accurately than with polymers used in traditional lithography owing to the higher hardness of the glass.

The mechanism of light-induced chemical interaction of Ag atoms with As₂S₃ matrix is based on the formation of Ag-S bonds on the surface of the film according to the following reactions:



We purposely omit specifying the charge state of the atoms in reactions (6) and (7). This is the subject of a separate study. Reactions (6) and (7) are only one part of the mechanism of photodissolution, which is a much more complicated time/dose-dependent process involving reversible changes, possible formation of an Ag-containing ternary, etc. A detailed explanation can be found elsewhere.⁴⁰ The confirmation of As separation at photodissolution is shown in Fig. 10, where the removal of As atoms in HNO₃ solution is demonstrated by the XPS data. The As-removal process progresses linearly with time of irradiation from a halogen lamp.

3 Ultrathin Fresnel Lenses on Chalcogenide Glass As₂S₃ Thin Films

The sulfur-based chalcogenide glasses can be made transparent in a wide wavelength range from visible up to more than 12 μm using an optimized chemical composition. While irradiation of ChG by light of band-gap energy and above ($\lambda < \lambda_g$, where λ_g is the wavelength corresponding to the band gap energy) may induce photostructural transformations accompanied by the change of optical

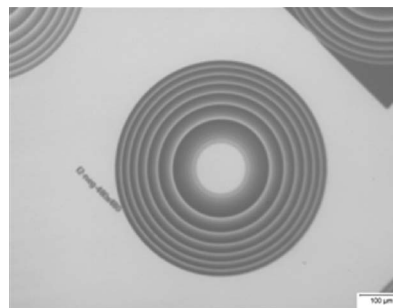


Fig. 11 Designed Fresnel lens mask on HEBS glass.

properties.²⁷ That is why the most promising functionality of grayscale features on ChG resists has been microlens arrays for infrared applications.^{8,9,26,41,42} For some applications in Si technology such as focal plane arrays for energy concentration or remote sensing, ultrathin (~600 nm) Fresnel lenses seem to be a very promising solution. They are capable of high focus (small focal length) with wide aperture (diameter of Fresnel lens) within a thin layer of material. Successful attempts to obtain Fresnel lenses on ChG thin films have already been made.⁴³⁻⁴⁵ However, either no optical characterization was reported or thickness of the lens layer was not particularly thin (>1.0 μm).

We selected the fabrication of a Fresnel lens and an array of similar lenses to demonstrate and establish the advantages of ChG as a material capable of forming complex optical structures in a single etching step. Aspheric (parabolic) height profile for the lens was calculated, assuming 2.35 as refractive index of ChG. The lens structure was designed for film thickness (i.e., maximum height of structure) of 600 nm, deposited on 475-μm-thick silicon wafer, with the intention to focus 10-μm radiation from the lens area to the backside of the wafer. Such design allows direct application of the ultrathin lenses in MEMS and silicon technology. The resulting height profile was assigned to 256 levels of gray, presuming linear dependency of gray level to final height transfer and all intermediate transfers. It was then converted to scalable vector graphics (SVG) format using a specially developed program in the BASH scripting language. The SVG file was designed with 2048 individual ringlets for high precision. We reduced the resulting data file to a grayscale bitmap with 480 × 480 pixels, using bicubic resampling, and extracted pixels corresponding to eight ranges of gray levels. The eight bins/ranges for extraction were selected to be linear in the original 256 gray levels, and extraction was performed by a specially developed PYTHON program that can be used to process any bitmap to any number of bins. The output of this program was converted to filled rectangles as required using nanometer pattern generation system (NPGS) electron lithography (<http://www.jcnabity.com>), which uses DesignCAD LT 2000 as the plotting program. This method was selected due to inherent limitations of the most common lithographic data format, GDS-II, and due to the limitations of the NPGS system.

A high-energy beam-sensitive (HEBS) blank glass mask was exposed to form the resulting NPGS pattern by electron beam, using a LEO 1550 VT electron microscope, op-

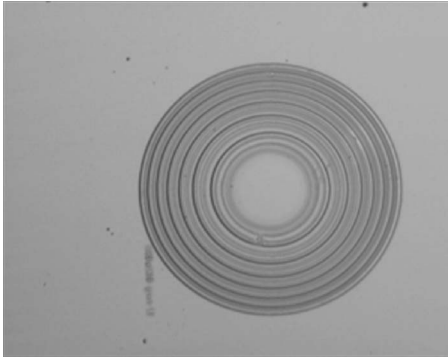


Fig. 12 Optical micrograph of Fresnel lens (thickness 600 nm) made of As_2S_3 film on silicon substrate.

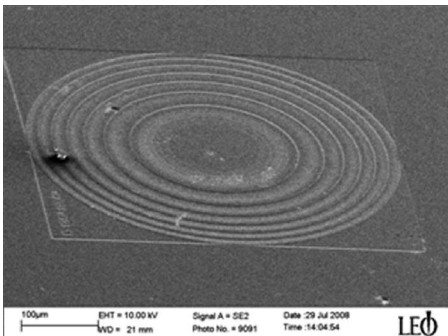


Fig. 13 SEM image of Fresnel lens made of As_2S_3 (thickness 600 nm) on silicon substrate.

erating at 30-kV acceleration voltage, with 20 Pa of N_2 residual pressure to avoid charging. Each polygon was selected to cover the area of 980×980 nm to avoid accidental overlap. Polygons were composed by points, each having center-to-center distance and line distance of

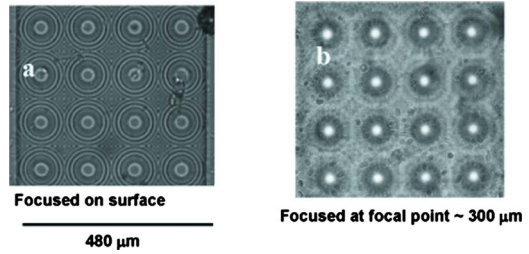


Fig. 15 Optical characterization of Fresnel lens array on glass substrate: lens focused on the surface (a) and at the focal point (b).

approximately 48 nm. Corresponding area dose was selected to be 0, 40, 80, 120, 160, 200, 240, and $280 \mu\text{C}/\text{cm}^2$ for each of the respective gray levels. The beam current was measured prior to and after writing, using a Faraday cup in the scanning electron microscope (SEM) chamber. A number of grayscale masks with lens structures were inspected by optical microscope, as shown in Fig. 11. There are no visible digital artifacts, although only eight exposure levels (corresponding to eight bins for original grayscale) and 480×480 rectangles were used. After inspection and cleaning in a clean room, the mask was used for exposing the ChG film by contact lithography. The mask contained two types of Fresnel lens structures: individual lenses of $400 \mu\text{m}$ diameter (Fig. 11) and arrays of lenses ($480 \times 480 \mu\text{m}^2$) that consist of 16 lenses each.

To develop ultrathin Fresnel lenses on ChG, thin films of As_2S_3 were deposited onto glass and silicon substrates via high vacuum thermal evaporation–deposition. Optimum conditions for film formation on silicon wafers were established first by depositions on a test glass substrate. Next, the As_2S_3 film was exposed through the mask to 365-nm wavelength light of intensity $8.4 \text{ mW}/\text{cm}^2$ using a Karl SUSS MA-6 mask aligner in the clean room and then etched with a nonaqueous amine-based solvent. Suitable duration of irradiation and conditions of etching were es-

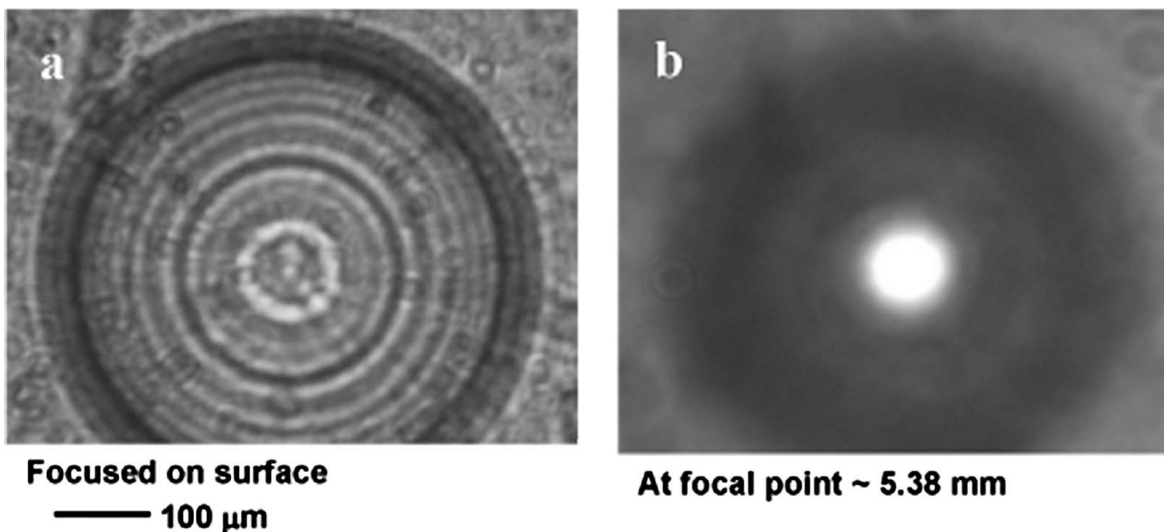


Fig. 14 Optical characterization of individual Fresnel lens ($400 \mu\text{m}$ diameter, 600 nm thickness) on glass substrate: microscope lens focused on the surface (a) and at the focal point that is 5.38 mm from the surface (b).



Fig. 16 CCD camera images of the beam focused by Fresnel lens on Si substrate (a), passing through plain ChG film on Si substrate (b) and direct laser beam (c). The scale bar in (a) is applicable to both (b) and (c).

tablished. Fresnel lenses were designed so that when etched into a chalcogenide film on a silicon substrate, the light would focus at a point on the back of the silicon wafer. The resulting lenses were examined under an optical microscope (Fig. 12) and SEM (Fig. 13) to determine whether the mask's grayscale integrity was maintained in the etched samples.

To determine whether the lenses had any optical functionality, the focal length of the Fresnel lenses was measured using an optical microscope in transmission mode with the condenser removed. As the microscope objective is moved away from the top surface of the lensed substrate, the observed light cone decreases to a minimum radius above which it again increases. The position of the minimum radius is taken as the focal point of the lens, and we report the focal length as the distance between the top surface of the lens and the position of minimum light cone radius. The pictures of the individual Fresnel lens of $400\ \mu\text{m}$ diameter focused on the surface (a) and at the focal point (b) are shown in Fig. 14. The focal length of the lenses is $5.38\ \text{mm}$ and differs slightly from the calculated value, probably because of the error introduced by the not fully optimized wet-etching step. The focal length for the Fresnel lenses within the $480 \times 480\ \mu\text{m}^2$ (Fig. 15) arrays is measured to be $\sim 300\ \mu\text{m}$, which is much closer to the calculated value.

The lens deposited on the silicon substrate was characterized using a laser beam from an infrared laser ($\lambda = 1.55\ \mu\text{m}$) and charge-coupled device (CCD) camera. The light from the laser was directed on the unpolished side of the Si wafer, while the lens, which was developed on the opposite polished side, was placed facing the camera. As

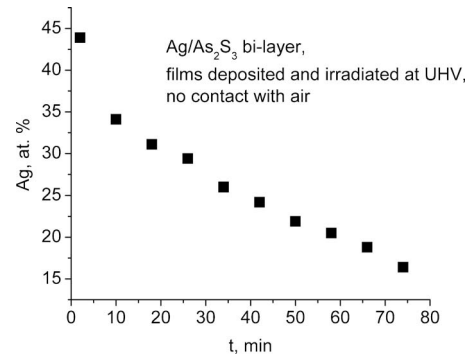


Fig. 17 XPS data on change of Ag concentration on the surface of As_2S_3 thin film with time of x-ray irradiation.

we can see from Fig. 16(a), the clear lens effect is observed, confirming optical functionality of the Fresnel lens. For comparison, Fig. 16(b) shows light through a flat As_2S_3 thin film, while Fig. 16(c) presents a CCD image of the laser beam without the sample.

4 Grayscale Lithography Based on Silver Photodissolution in Chalcogenide Glass Thin Films

The dissolution of silver in ChG thin films subjected to light, electron, or x-ray (Fig. 17) irradiation significantly changes its chemical resistance because of the gradual change of chemical composition. Grayscale photolithography in ChG is based on the fact that both the exposure time and the light intensity affect the etching rate. Figure 18 (right) shows the graph demonstrating the change of etched depth with increasing transparency of the grayscale features in a reference HEBS glass mask (left part of Fig. 18, line A-A') uniformly exposed by halogen lamp light. The optical density through the mask ranged from 0.126 (shallowest etch of 65 nm) to 0.217 (deepest etch of 230 nm), allowing variation of the light intensity on the glass surface. This dependence is close to linear, thus demonstrating dissolution of silver to different depths that depend on the total dose of irradiation as determined by the intensity and time

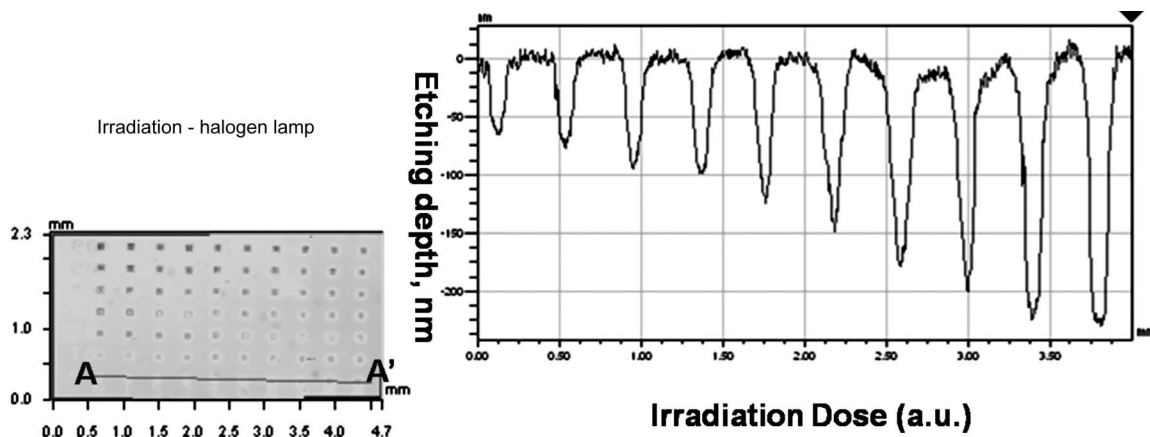


Fig. 18 Change of etching depth of $\text{Ag}/\text{As}_2\text{S}_3$ thin film layer with gradual variation of transparency of HEBS glass mask fragments.

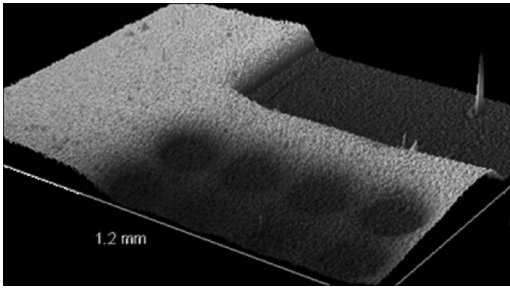


Fig. 19 Complex grayscale structure, obtained from Ag/As₂S₃ layer by negative RIE in CF₄ plasma.

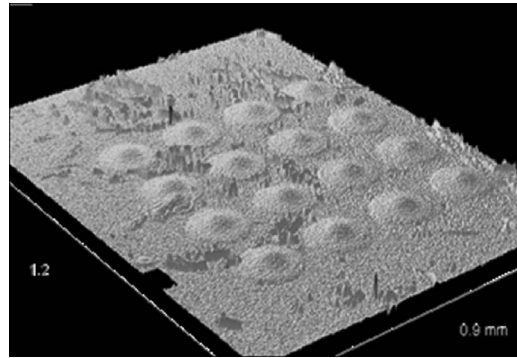


Fig. 20 Positive lens structure obtained by negative RIE in CF₄ plasma after prolonged irradiation of Ag/As₂S₃ layer.

of irradiation. So a smooth, predictable shaping of more complex patterns from the grayscale optical mask is expected. The selectivity of etching (defined as the etching rate ratio of exposed and unexposed regions of a sample) is a function of glass film composition, its prehistory, as well as the composition of etching gas. In our experiment, the etching depth was ~200 nm, although larger values are possible.

Increased chemical resistance of ChG thin films after Ag dissolution offers an opportunity to exploit the DRIE procedure for grayscale lithography. In this case, several additional variables influence the process, including gas composition, gas pressure, gas flow rates, substrate temperature,

electric power, and etch time. Other variables independent of etching method are film thickness, light intensity, and exposure time.

For demonstrating grayscale patterning, the ChG thin film samples were irradiated with a halogen lamp (Fiber-Lite PL-Illuminator, Dolan-Jenner Industries) through a HEBS5 calibration plate containing grayscale features with gradual smooth change of transparency as well as lens-like structures. The time of exposure was varied widely from 1 to 200 min. After exposure, the residual undiffused silver was removed from unexposed parts using dilute HNO₃.

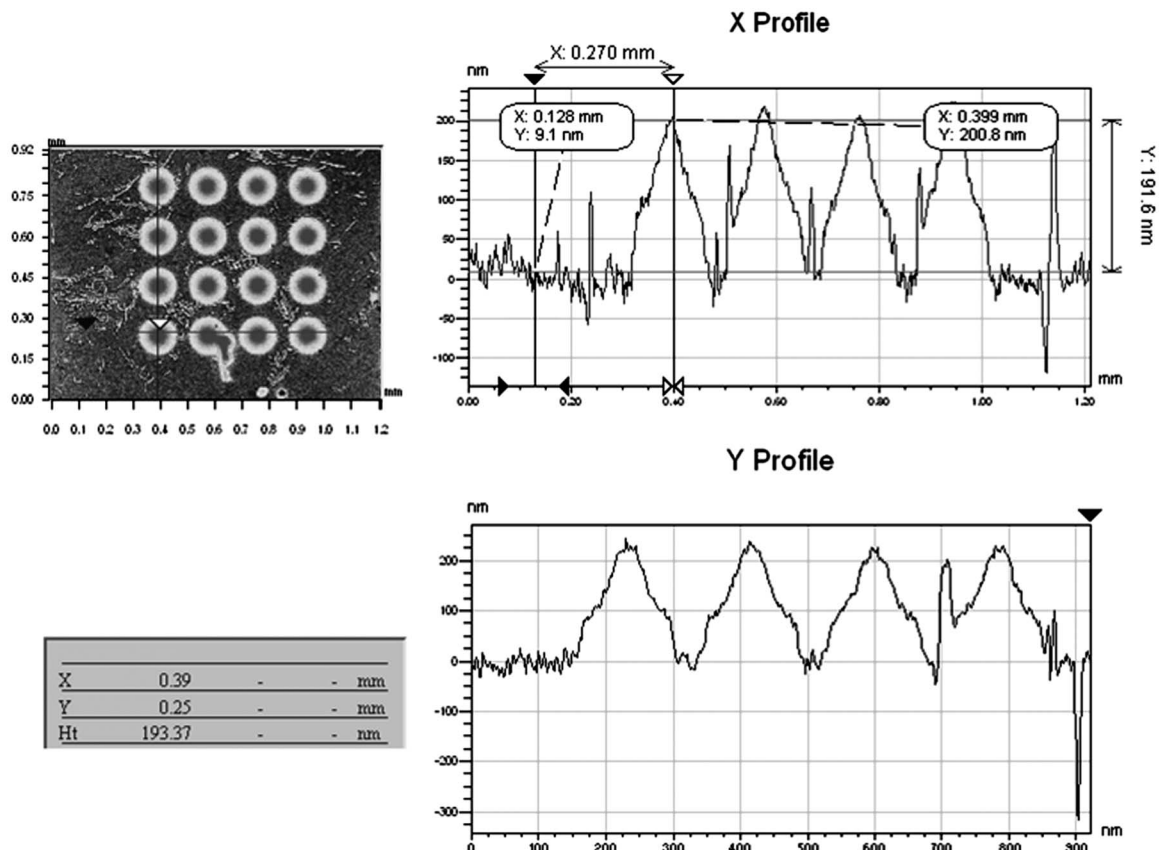


Fig. 21 Etch depth of the positively developed lens structures on Ag/As₂S₃ layers (after RIE in CF₄ plasma).

Dry etching was carried out with a parallel-plate RIE system (Plasma Therm SSL-720) using CF_4 as the etchant gas. A typical etch recipe consisted of chamber pressure, electrode power, CF_4 flow rate, and etch time of 100 mTorr, 110 W, 100 sccm, and 2 min, respectively. Pieces of the samples were mounted on unmasked 4-in Si wafer substrates using thermal grease (Cool-Grease TM 7016, AI Technology, Inc.) in order to utilize the load lock on the RIE system. The variation of etch depth was measured and imaged using a VEECO NT1100 optical profiler.

Depending on the time of irradiation, we were able to obtain negative or positive patterns. A section of complex grayscale structures, which was obtained by negative etching, is shown in Fig. 19. In this case, the duration of irradiation by halogen lamp through grayscale mask was 2 min. The significant increase of irradiation time resulted in switching from negative to positive etching (Fig. 20), probably due to the cascade of chemical reactions leading to the formation of Ag-enriched phase on the surface of the sample. The quality of the positive pattern is not as good as in the case of negative etching, indicating that the uniformity of the surface is worse in the case of Ag-enriched composition. However, the observed switching from negative to positive etching simply by varying the irradiation time of Ag/ As_2S_3 layer is a promising new parameter for controlling grayscale patterning.

Measurements of the etch depth of the positive features reveal that the average roughness of this pattern is ~ 50 nm (Fig. 21). This value is unacceptably high for submicron lithography. We believe that its origin is in the distinct phase separation upon prolonged irradiation. In the case of our negative patterns presented in Fig. 18, the average roughness usually is only a few nm and does not exceed the 20-nm level.

The exploratory experiments to transfer the grayscale patterns into Si substrate via RIE have given very encouraging results with an etch selectivity of $\sim 10:1$ (etch rate in Si/etch rate in ChG film), which is a large increase over conventional polymer masking materials with an etch selectivity in parallel-plate RIE below 2:1 for anisotropic etch profiles using a similar etch recipe. The etch selectivity with our ChG-Ag photoresist is likely to be further improved by the optimization of surface composition and RIE parameters and decreased silicon loading by masking the carrier wafer. The higher etch selectivity of ChG/silver films over traditional polymer films is believed to be due to the increase in hardness from Ag photodiffusion, which reduces the rate of physical sputtering by the energized ions responsible for RIE.

5 Conclusions

Chalcogenide glass thin films are promising materials for use as high-resolution, grayscale photo- and electron-beam resists for nanoscale and ultrathin applications in MEMS/NEMS technology. They can be patterned directly to form IR transparent thin film lens arrays, Fresnel lenses, diffractive optical elements, etc. The fabricated ultrathin Fresnel lenses demonstrate desired optical functionality. Photo-induced silver dissolution in ChG thin films introduces a new method for grayscale micropatterning. Nearly linear dependence of the etch depth on the total dose of absorbed

light suggests that high-quality 3-D patterning can be accomplished by dry reactive ion etching. Exploratory results show that the etch selectivity for transferring patterns into silicon is significantly superior to commonly used polymer resists used in lithography; process optimization should increase this ratio significantly.

Acknowledgments

Separate parts of this work were supported by the Center for Optical Technology (Lehigh University), a Lehigh University–Army Research Lab (ARL) collaborative research program; the National Science Foundation (DMR 00-74624, and DMR 03-12081, DMR 04-09588); and the Pennsylvania Department of Community and Economic Development through the Ben Franklin Technology Development Authority. M.V. thanks the Czech Ministry of Education, Youth, and Sports for support under Grant No. 0021627501.

References

1. E.-B. Kley, "Continuous profile writing by electron- and optical lithography," *Microelectron. Eng.* **34**, 261–298 (1997).
2. J. D. Rogers, A. H. O. Kärkkäinen, T. Tkaczyk, J. T. Rantala, and M. R. Descour, "Realization of refractive microoptics through grayscale lithographic patterning of photosensitive hybrid glass," *Opt. Express* **12**(7), 1294–1303 (2004).
3. I. B. Divliansky and E. G. Johnson, "Three-dimensional diffractive micro- and nano-optical elements fabricated by electron-beam lithography," *Proc. SPIE* **6462**, 64621B1–64621B8 (2007).
4. C. M. Waits, A. Modafe, and R. Ghodssi, "Investigation of gray-scale technology for large area 3D silicon MEMS," *J. Micromech. Microeng.* **13**(2), 170–177 (2003).
5. T. Nachmias, A. Ohayon, S. E. Melzer, M. Kabla, E. Louzon, and U. Levy, "Shallow Fresnel lens fabrication using grayscale lithography made by high energy beam sensitive mask (HEBS) technology and reactive ion etching," *Proc. SPIE* **7205**, 72050B1–72050B12 (2009).
6. B. Morgan, C. M. Waits, J. Krizmanic, and R. Ghodssi, "Development of a deep silicon phase Fresnel lens using gray-scale lithography and deep reactive ion etching," *J. Microelectromech. Syst.* **13**(1), 113–120 (2004).
7. K. Hanai, T. Nakahara, S. Shimizu, and Y. Matsumoto, "Fabrication of three-dimensional structures by image processing," *Sens. Mater.* **18**(1), 49–61 (2005).
8. H. Jain and M. Vlcek, "Glasses for lithography," *J. Non-Cryst. Solids* **354**, 1401–1406 (2008).
9. A. Kovalskiy, M. Vlcek, H. Jain, A. Fiserova, C. M. Waits, and M. Dubey, "Development of chalcogenide glass photoresists for grayscale lithography," *J. Non-Cryst. Solids* **352**, 589–594 (2006).
10. V. Lyubin, "Chalcogenide glassy photoresists: history of development, properties, and applications," *Phys. Status Solidi B* **246**, 1758–1767 (2009).
11. E. V. Berlin, B. T. Kolomiets, V. M. Lyubin, S. I. Nesterov, V. V. Rudnev, and V. P. Shilo, "X-ray stimulated structural transformations in amorphous chalcogenide semiconductors," *Sov. Tech. Phys. Lett.* **7**, 654–655 (1981).
12. G. B. Hoffman, W.-C. Liu, W. Zhou, R. Sooryakumar, P. Boolchand, and R. M. Reano, "Relief and trench formation on chalcogenide thin films using electron beams," *J. Vac. Sci. Technol. B* **26**, 2478–2483 (2008).
13. S. Schroeter, M. Vlcek, R. Poehlmann, and A. Fiserova, "Efficient diffractive optical elements in chalcogenide glass layers fabricated by direct DUV laser writing," *J. Phys. Chem. Solids* **68**, 916–919 (2007).
14. J. Wei and X. Jiao, "Super-resolution nanopatterns and optical recording in chalcogenide phase change thin films by direct laser writing," *Proc. SPIE* **7125**, 712505 (2008).
15. A. Zoubir, M. Richardson, C. Rivero, A. Schulte, C. Lopez, K. Richardson, N. Ho, and R. Vallee, "Direct femtosecond laser writing of waveguides in As_2S_3 thin films," *Opt. Lett.* **29**, 748–750 (2004).
16. E. Nicoletti, G. Zhou, B. Jia, M. J. Ventura, D. Bulla, B. Luther-Davies, and M. Gu, "Observation of multiple higher-order stopgaps from three-dimensional chalcogenide glass photonic crystals," *Opt. Lett.* **33**, 2311–2313 (2008).
17. A. Bulanovs, V. Gerbrederis, V. Paschkevich, and J. Teteris, "Dot-

- matrix holographic recording in amorphous chalcogenide films," *Proc. SPIE* **6596**, 65960K (2006).
18. J. R. Neilson, A. Kovalskiy, M. Vlcek, H. Jain, and F. Miller, "Fabrication of nano-gratings in arsenic sulphide films," *J. Non-Cryst. Solids* **353**, 1427–1430 (2007).
 19. M. Vlcek and H. Jain, "Nanostructuring of chalcogenide glasses using electron beam lithography," *J. Optoelectron. Adv. Mater.* **8**, 2108–2111 (2006).
 20. Z. U. Borisova, *Glassy Semiconductors*, Plenum Press, New York and London (1981).
 21. P. G. Huggett, K. Frick, and H. W. Lehmann, "Development of silver sensitized germanium selenide photoresist by reactive sputter etching in SF₆," *Appl. Phys. Lett.* **42**, 592–594 (1983).
 22. P. F. Romanenko, I. I. Robur, A. V. Stronski, I. Z. Indutnyi, P. E. Schepelyavi, S. A. Kostioukevitch, and L. A. Kostrova, "Holographic optical elements, holograms production on the base of chalcogenide vitreous semiconductor layers," *Proc. SPIE* **2108**, 110–114 (1993).
 23. K. L. Chopra, L. K. Malhotra, K. S. Harshavardhan, and S. Rajagopalan, "Photon, electron, and ion beam induced physical and optical densification in chalcogenide films," *Bull. Mater. Sci.* **6**, 1013–1018 (1984).
 24. P. K. Gupta, A. Kumar, L. K. Malhotra, and K. L. Chopra, "Plasma-processed positive and negative resist behavior of obliquely deposited amorphous P-Se films," *J. Vac. Sci. Technol. B* **3**, 1590–1593 (1985).
 25. M. Vlcek, J. Prokop, and M. Frumar, "Positive and negative etching of As-S thin layers," *Int. J. Electron.* **77**(6), 969–973 (1994).
 26. N. P. Eisenberg, M. Manevich, S. Noach, M. Klebanov, and V. Lyubin, "New types of microlens arrays for the IR based on inorganic chalcogenide photoresists," *Mater. Sci. Semicond. Process.* **3**(5–6), 443–448 (2000).
 27. W. Li, Y. Ruan, B. Luther-Davies, A. Rode, and R. Boswell, "Dry-etch of As₂S₃ thin films for optical waveguide fabrication," *J. Vac. Sci. Technol. A* **23**(6), 1626–1632 (2005).
 28. O. I. Shpotyuk, "Photostructural transformations in amorphous chalcogenide semiconductors," *Phys. Status Solidi B* **183**(2), 365–374 (1994).
 29. A. V. Kolobov, B. T. Kolomiets, O. V. Konstantinov, and V. M. Lyubin, "A model of photostructural changes in chalcogenide vitreous semiconductors. I. Theoretical considerations," *J. Non-Cryst. Solids* **45**(3), 335–341 (1981).
 30. V. L. Averyanov, A. V. Kolobov, B. T. Kolomiets, and V. M. Lyubin, "A model of photostructural changes in chalcogenide vitreous semiconductors. II. Experimental results," *J. Non-Cryst. Solids* **45**(3), 343–353 (1981).
 31. S. A. Zenkin, S. B. Mamedov, M. D. Mikhailov, E. Yu. Turkina, and I. Yu. Yusupov, "Mechanism for interaction of amine solutions with monolithic glasses and amorphous films in the As-S system," *Glass Phys. Chem.* **23**(5), 393–399 (1997).
 32. M. Vlcek, M. Frumar, M. Kubovy, and V. Nevsimalova, "The influence of the composition of the layers and of the inorganic solvents on photoinduced dissolution of As-S amorphous thin films," *J. Non-Cryst. Solids* **137–138**, 1035–1038 (1991).
 33. M. Hattori, H. Suzuki, and Y. Enoki, "Heats of solution of As-S, As-Se, and As-S-Se glasses in alkaline solutions," *J. Non-Cryst. Solids* **52**, 405–411 (1982).
 34. B. C. Bostick, S. Fendorf, and G. E. Brown Jr., "In situ analysis of thioarsenite complexes in neutral to alkaline arsenic sulphide solutions," *Miner. Mag.* **69**(5), 781–795 (2005).
 35. P. Lucas, A. A. Wilhelm, M. Videau, C. Boussard-Pledel, and B. Bureau, "Chemical stability of chalcogenide infrared glass fibers," *Corros. Sci.* **50**(7), 2047–2052 (2008).
 36. J. Orava, T. Wagner, M. Krbal, T. Kohoutek, M. Vlcek, and M. Frumar, "Selective wet-etching of undoped and silver photodoped amorphous thin films of chalcogenide glasses in inorganic alkaline solutions," *J. Non-Cryst. Solids* **352**, 1637–1640 (2006).
 37. V. Balan, C. Vigreux, A. Pradel, A. Llobera, C. Dominguez, M. I. Alonso, and M. Garriga, "Chalcogenide glass-based rib ARROW waveguide," *J. Non-Cryst. Solids* **326–327**, 455–459 (2003).
 38. H.-Y. Lee and H.-B. Chung, "Low-energy focused-ion-beam exposure characteristics of an amorphous Se₇₅Ge₂₅ resist," *J. Vac. Sci. Technol. B* **15**(4), 818–822 (1997).
 39. D. Freeman, C. Grillet, M. W. Lee, C. L. C. Smith, Y. Ruan, A. Rode, M. Krolkowska, S. Tomljenovic-Hanic, C. M. de Sterke, M. J. Steel, B. Luther-Davies, S. Madden, D. J. Moss, Y.-H. Lee, and B. J. Eggleton, "Chalcogenide glass photonic crystals," *Photonics Nanostruct. Fundam. Appl.* **6**, 3–11 (2008).
 40. H. Jain, A. Kovalskiy, and A. Miller, "An XPS study of the early stages of silver photodiffusion in Ag/a-As₂S₃ films," *J. Non-Cryst. Solids* **352**, 562–566 (2006).
 41. A. Saitoh, T. Gotoh, and K. Tanaka, "Chalcogenide-glass microlenses attached to optical-fiber end surfaces," *Opt. Lett.* **25**(24), 1759–1761 (2000).
 42. J. G. Smith and G. T. Borek, "Etching of chalcogenide glass for IR microoptics," *Proc. SPIE* **6940**, 69400W (2008).
 43. A. V. Stronski, "Application of As-S-Se chalcogenide inorganic resists in diffractive optics," *Proc. SPIE* **3729**, 250–254 (1999).
 44. N. P. Eisenberg, M. Manevich, A. Arsh, M. Klebanov, and V. Lyubin, "New micro-optical devices for the IR based on three-component amorphous chalcogenide photoresists," *J. Non-Cryst. Solids* **352**, 1632–1636 (2006).
 45. I. Z. Indutnyi, A. V. Stronski, S. A. Kostioukevitch, P. F. Romanenko, P. E. Schepeljavi, and I. I. Robur, "Holographic optical element fabrication using chalcogenide layers," *Opt. Eng. (Bellingham)* **34**, 1030–1039 (1995).



Andriy Kovalskiy received BS and MS degrees in electronics and a PhD in solid-state physics from Lviv State University (Ukraine). He joined the Center for Optical Technologies at Lehigh University in 2004 as a research associate. For the past five years, he has worked on the development of novel grayscale photoresists and fabrication of ultrathin Fresnel lenses in chalcogenide glass thin films. He has published over 50 papers in peer-reviewed journals and presented more than 150 conference contributions. His other research interests include surface physics, atomic and electronic structures (high-resolution XPS, EXAFS, NEXAFS), photo- and radiation-induced effects in glasses and thin films, and applications of chalcogenide glasses.



Jiri Cech graduated from the University of Pardubice, Czech Republic, where his thesis, "Forming of diffractive microoptical elements in amorphous chalcogenide thin films," was awarded best in class of 2002. Between 2002 and 2006, he worked in the group of Prof. Klaus von Klitzing, in the molecular electronics and carbon nanotubes section at the Max Planck Institute for Solid State Research at Stuttgart, Germany. In 2006, he joined Lehigh University, where he worked on the design and fabrication of an ultra-thin Fresnel lens array in chalcogenide glass and a freestanding CNT-based microbolometer prototype. He is the author of over 20 peer-reviewed publications. Currently, he is working at DTU Nanotech, Department of Micro- and Nanotechnology, Technical University of Denmark.



Miroslav Vlcek is a professor of inorganic chemistry at the University of Pardubice, Czech Republic. He has studied the physicochemical properties and structure of chalcogenide glasses (ChG) since 1981. His recent research has focused on photo-induced structural changes in these materials, which affect their optical properties and chemical resistance. He has exploited these phenomena for the development of new high-resolution photoresists for grayscale lithography and nanopatterning using electron-beam lithography, especially in diffractive optics, optoelectronics, high-resolution lithography, fabrication of counterfeiting elements, etc. Presently, he is exploring the possibility of microstructuring of chalcogenide glass by direct laser writing, which would allow fabrication of submicron 3-D structures without any wet/dry etching. He is the author of more than 90 peer-reviewed papers in international journals.



Christopher M. Waits received a BS in physics from Salisbury University, Maryland, in 2000, and MS and PhD degrees in electrical engineering from the University of Maryland, College Park, in 2003 and 2008, respectively. In 2000, he received a Physics Excellence Award from Salisbury University, and from 2001 to 2003, he was awarded a Graduate Assistance in Areas of National Need (GAAN) fellowship. He joined the Sensors and Electron Devices Directorate

at the U.S. Army Research Laboratory, Adelphi, Maryland, as an electronics engineer in 2004. In 2007, he received the Department of the Army Research and Development Achievement Award for Technical Excellence. His main research interests include MEMS components and systems for power and energy generation and conversion (Power MEMS), MEMS tribology and bearing mechanisms, and new microfabrication techniques.



Madan Dubey is a research physical scientist and team leader at the Nanoelectronics, Sensors, and Electron Devices Directorate, U.S. Army Research Laboratory, Aberdeen, Maryland. He is responsible for the fundamental research concerning the concepts, phenomena, and methodology associated with nano/microelectromechanical systems, especially the development of new processes for making piezoelectric MEMS devices. He is also responsible for the implementation of program objectives and for conducting reviews to

achieve cross-functional integration and maximum exploitation of technologies available in industry and other international sources.



William R. Heffner has been associate director of the International Materials Institute for New Functionality in Glass at Lehigh University since 2004. In this position, he facilitates research exchanges promoting new functionality in glass. He is developing an e-based glass learning curriculum for the glass research community as well as hands on experiments for young science enthusiasts. Previously, he was with AT&T Bell Laboratories and Agere Systems as a distinguished member of the technical staff, with 25 years of experience in optoelectronic device research and development. He has taught courses on lasers and optoelectronic device physics at Penn State University and created an optoelectronics training curriculum for Agere employees. He received an MS in chemical physics from Indiana University and a PhD in physics from Stevens Institute of Technology. He has 17 publications and 6 patents on optical devices.

in glass through fundamentals; point defects, electrical relaxation, conductivity, and dielectric properties of amorphous and crystalline ceramics; light-induced phenomena in glass; glasses for IR biosensors, photo- and nanolithography, and photonics; tailored transparent ferroelectric nanocomposites; nano-macro porous glass for bone-scaffolds; and surface conduction.



Himanshu Jain is the T. L. Diamond Distinguished Chair in Engineering and Applied Science, a professor of materials science and engineering, and the director of NSF's International Materials Institute for New Functionality in Glass at Lehigh University. Previously, he conducted research at Argonne and Brookhaven National Laboratories. An author of over 260 publications, he is a fellow of the American Ceramic Society. His research interests include functionality

in glass through fundamentals; point defects, electrical relaxation, conductivity, and dielectric properties of amorphous and crystalline ceramics; light-induced phenomena in glass; glasses for IR biosensors, photo- and nanolithography, and photonics; tailored transparent ferroelectric nanocomposites; nano-macro porous glass for bone-scaffolds; and surface conduction.